

1 **Reviewer #1:**

2 This study focuses on balloon measurements carried out from the Tibetan plateau to understand
3 the microphysical processes involved in aerosol formation and growth in the Upper Troposphere
4 and Lower Stratosphere during the Summer Asian Monsoon. The authors use the COBALD
5 backscatter sonde together with the Cryogenic Frost Point Hygrometer to understand how
6 humidity affects the size of aerosols. In addition, they use Mie calculations to interpret those
7 measurements. Overall, the paper is short, to the point, well written and follow a logical path with
8 clear figures and consistent interpretation. I would recommend the publication of this manuscript
9 in ACP after the following points are corrected :

10

11 - P1-L27 replace “a balloon..” by “the balloon..”

12 **R: Done.**

13

14 - P1-L28 add “COBALD sensor”

15 **R: We rewrote the sentence as ‘using the balloon-borne, lightweight Compact Optical Backscatter**
16 **Aerosol Detector (COBALD) instruments above Linzhi’ according to the comments from the two**
17 **reviewers..**

18

19 - P2L20: Park et al. [2007] should not be quoted here but rather after “large scale circulation..”

20 **R: Done.**

21

22 - P3L6. Frey et al. [2011] talk about the West African Monsoon and the Asian Monsoon.

23 Do you think it’s relevant here ?

24 **R: We agreed with reviewer’s concerns and rewrote this and related sentence earlier as**
25 **‘Sources and formation mechanism of aerosols in the UTLS, especially over the tropics, have been**
26 **studied over the past decades. New particle formation events can occur at very low temperatures**
27 **accompanied by the outflow of convective systems, as observed in the West African Monsoon [Frey**
28 **et al., 2011]’. Here we merely give a brief overview about the studies for the UTLS.**

29

30 - P7L7. Are you sure that the Kelud eruption did not impact those balloon measurements?

31 **R: We appreciate the reviewer’s suggestions (also from Reviewer #2) and add the**
32 **corresponding discussion about the Kelud eruption.**

33 *‘On February 13, 2014 the Mt. Kelud (8°S, 112°E) in Indonesia erupted, with a volcanic plume*
34 *located near 18-21 km within the tropical stratosphere, which was detected 11 days after the*
35 *eruption by the Cloud-Aerosol Lidar with Orthogonal Polarization (CALIOP) onboard the Cloud-*
36 *Aerosol Lidar and Infrared Pathfinder Satellite Observation (CALIPSO) [Vernier et al, 2016].*
37 *Stratospheric aerosols were perturbed significantly by the Kelud volcanic plumes, especially the*
38 *fresh ash plume in the southern hemisphere [Vernier et al, 2016; Sakai et al., 2016], The Kelud*
39 *volcanic eruption might have negligible influence on the observed aerosols in the ATAL, since the*
40 *ATAL began to form about four months after the Kelud eruption when the volcanic materials in the*
41 *troposphere might have vanished. On the other hand, CALIOP data analysis also showed that*
42 *sulfate components from the Kelud volcanic eruption, peaking at an higher altitude with a longer*
43 *residence time compared with the volcanic ashes, influenced aerosol optical depth (AOD) between*
44 *20°N and 20°S 18-25 km considerably three months after the eruption [Vernier et al, 2016]. It is*

1 likely that sulfate aerosols from the Kelud eruption contributed to stratospheric background
2 aerosols above the ATAL and even in the Junge layer at slightly higher latitude, as indicated by our
3 COBALD measurements’.

4
5 - Fig.1. I would rather differentiate in this plot: the Junge Layer, the stratospheric aerosol layer
6 peaking in the mid stratosphere and the ATAL which is limited to the Upper Tropospheric and
7 Lower Stratospheric region.

8 **R: We appreciate the reviewer’s suggestions and add the corresponding statement about the
9 enhanced aerosol layer from COBALD measurement in the first paragraph of Sect. 3.**

10 *“The enhanced aerosol layer from COBALD measurement is a mixture of ATAL and the on-
11 setting Junge Layer due to the signal above 50 hPa stemming from the Junge Layer but the
12 maximum occurring in ATAL”.*

13
14 - Fig.2. Here, it’s important to define the lower size boundary that cannot be observed
15 by COBALD due to the lack of scattering efficiency of small aerosols. I would say that
16 30-40 nm is probably the limit.

17 **R: We agreed with reviewer’s concerns and added the corresponding statement and a new
18 table about the lower size boundary of COBALD measurement.**

19 *“The signal to noise ratio at the blue channel with respect to the molecular Rayleigh backscatter at
20 tropopause conditions (taken 100 hPa and 210 K) is 220. Given the molecular backscatter
21 coefficient of $4.4e^{-7}$ ($sr^{-1}m^{-1}$) for 455 nm, this corresponds to a backscatter coefficient minimum
22 detection limit of $2e^{-9}$ ($sr^{-1}m^{-1}$), which is holding in general over the entire profile. To define an
23 aerosol size limit, typical aerosol number densities need to be assumed: 10 cm^{-3} for stratospheric
24 background and 100 cm^{-3} for the ATAL. The aerosol backscatter coefficients of different aerosol
25 mode radius for the typical aerosol number densities are calculated by Mie theory and listed in
26 Table 1. The results confirm that the particles with 100 nm radius are well detected under
27 background conditions, which mainly contribute to the particulate backscatter ratio of approx. 0.01
28 and is always present. With increasing particle number density, the particles with 30 nm radius
29 start to contribute to the particulate backscatter ratio ($> 2e^{-9}\text{ sr}^{-1}m^{-1}$). Therefore, the lower size
30 boundary that cannot be observed by COBALD due to the lack of scattering efficiency of small
31 aerosols can be defined as 30 nm.*

32
33 **Table 1** The aerosol backscatter coefficients of different aerosol mode radius for the typical aerosol
34 number densities.

Mode Radius (nm)	10	30	100
$\beta_a@10\text{ cm}^{-3}$ ($sr^{-1}\text{ m}^{-1}$)	$1e^{-12}$	$3e^{-10}$	$2e^{-8}$
$\beta_a@100\text{ cm}^{-3}$ ($sr^{-1}\text{ m}^{-1}$)	$1e^{-11}$	$3e^{-9}$	$2e^{-7}$

35 ”

36
37 - Fig.3 was also explored in Vernier et al., 2015 (Fig.3) using the same technique. I
38 think it’s important to make sure that data plotted here are not in the stratosphere and

1 should remain below 19 km. The upper pressure limit (50 hPa) includes stratospheric
2 data and I believe that the points in black where CI is between 4-6 and RH_i below 40
3 % could be in the stratosphere. It would be interesting to color the points according to
4 their heights.

5 **R: We agreed with reviewer's concerns and replotted Fig 3b by coloring the points according**
6 **to the height of particles.**

7
8 More generally, the authors should remain the reader than the conclusions drawn from
9 this paper are only based on 3 balloon flights so that general conclusions should be
10 established with caution.

11 **R: The reviewer's comments are very valuable. We added a sentence about the conclusions**
12 **drawn from only 7 balloon flights.**

13 *"It must be borne in mind that the conclusions drawn from this study are only based on 7 balloon*
14 *flights so that general conclusions should be established with caution".*

15

1 **Reviewer #2:**

2 Overall, the manuscript is reasonably well written and logically constructed. The writing is
3 certainly understandable, but does exhibit some usage and punctuation errors. The topic is
4 appropriate for publication in ACP.

5 One general comment is on the use and discussion of ‘condensational growth’ in the context of
6 water uptake. While perhaps technically correct, it would be better to distinguish between
7 hygroscopic growth, a dynamic and typically reversible process, and growth of particles by
8 accretion of additional low volatility material (e.g. H₂SO₄ or SOA). It is noted in the manuscript
9 that ‘the growth mechanism of the particles in the ATAL is still poorly described’ and while the
10 authors discuss observed relationships between RH_i and the COBALD-derived aerosol
11 backscatter and color index, the phenomenology does not fully constrain the mechanisms. If the
12 elevated RH_i resulted in condensational growth through enhanced chemical production, the
13 observed relationship would break down since the dependence would be on RH_i history rather
14 than instantaneous RH_i as considered here.

15 **R: We thank Reviewer #2 for insightful comments and constructive suggestions! We agree**
16 **with reviewer’s concerns and have revised the manuscript accordingly as specified below.**

17

18 Specific comments:

19 Title: ‘condensational growth’ – see comment above

20 ‘over Tibetan Plateau’ >> ‘over the Tibetan Plateau’

21 **R: The title of this manuscript has been changed to ‘Observational evidence of particle**
22 **hygroscopic growth in the UTLS over the Tibetan Plateau’.**

23

24 P1L24: ‘Water plays an important role in the growth’ – see comment above. Water is
25 important in determining the size, and therefore radiative properties, of the particles.

26 **R: We rewrote this sentence as suggested by the reviewer.**

27

28 P1L27: ‘aerosol backscattering ratio’ >> ‘backscatter ratio’ more common and as it does appear
29 elsewhere in the manuscript. ‘aerosol’ is not appropriate here since the
30 acronym and numbers quoted subsequently are BSR, not ABSR = BSR – 1, as defined in the paper.
31 Alternately, ‘aerosol backscattering’ could be used here and ‘backscatter ratio’ added to BSR in
32 L30.

33 **R: We changed ‘aerosol backscattering ratio’ to ‘backscatter ratio’ as suggested by the**
34 **reviewer.**

35

36 P1L27: ‘with a balloon-borne lightweight COBALD at Linzhi’ – the profiles were measured with
37 separate COBALD instruments, so perhaps ‘using balloon-borne, lightweight COBALD instruments
38 above Linzhi’. I believe the COBALD acronym should technically be spelled out in the abstract as
39 well as the body (as UTLS is).

40 **R: We rewrote this sentence as ‘using the balloon-borne, lightweight Compact Optical**
41 **Backscatter Aerosol Detector (COBALD) instruments above Linzhi’ according to the comments**
42 **from both reviewers.**

43

44 P1L32: Here the CI is defined in terms of ABSR, but that is not defined—perhaps harmonize with

1 the BSR discussion earlier in the abstract.

2 **R: We rewrote this sentence according to this comment as well that for P1L27 about BSR.**

3

4 P2L1: delete 'dominant' >> 'indicating the prevalence of fine particles'

5 **R: Done.**

6

7 P2L6: as noted in the general comments above, water uptake at high RH is increasing the size of
8 the particles (hygroscopic growth), but it is not really the case that water vapor is playing 'a very
9 important role in the formation of large amounts of fine particles' unless you are considering the
10 role of H2O in aerosol nucleation, which is not something that is addressable through the
11 measurements in this study.

12 **R: We rewrote this phrase as 'water vapor can play a very important role in increasing the size
13 of fine particles'.**

14

15 P2L8: 'condensational growth' – see comment above

16 **R: We replaced 'condensational growth' with 'hygroscopic growth'.**

17

18 P2L9: 'enhancement' – hygroscopic growth would enhance the size, and therefore radiative
19 effects, of the ATAL aerosol, but is really not responsible for the ATAL formation.

20 **R: We rewrote this sentence as 'aerosol particle hygroscopic growth is an important factor
21 influencing the radiative properties of the Asian Tropopause Aerosol Layer (ATAL) during the Asian
22 summer monsoon'.**

23

24 P2L22: 'global warm effect from greenhouse gases.' >> 'global warming effect from increasing
25 greenhouse gas concentrations.'

26 **R: Done.**

27

28 P2L23: 'maximum' >> 'elevated' (also in L27)

29 **R: Done.**

30

31 P3L5: '[Frey et al., 2011] proposed' >> 'Frey et al. [2011] proposed'

32 **R: This sentences has been changed as 'New particle formation events can occur at very low
33 temperatures accompanied by the outflow of convective systems, as observed in the West African
34 Monsoon [Frey et al., 2011]' according to the comment from Reviewer #1.**

35

36 P3L9: 'after the relative humidity' – after it what? This sentence could be restructured to be
37 clearer. Also, CALIOP is the lidar, CALIPSO is the satellite.

38 **R: We meant a one-month phase lag of the starting point of increase in aerosol scattering ratio
39 after the starting point of increase in relative humidity. Anyhow, we deleted this sentence
40 considering that it dose not contribute to the core of the argument in this paper, as pointed out
41 by the reviewer.**

42

43 P3L8-12: related to the question of the use of 'condensational growth', I am unclear what is
44 being proposed as the mechanism by which increased relative humidity would take one month

1 to affect the size of aerosol. Beyond the role of H₂O in the formation of molecular (or ion-
2 molecule) clusters that can subsequently grow into aerosols, it would take significant
3 supersaturations for sufficient water to condense on nanometer sized (nucleation mode)
4 particles to produce growth, and then it would likely produce activation to large size (cloud). This
5 could theoretically lead to growth of the underlying particles through aqueous chemistry (e.g.
6 SO₂ & H₂SO₄), resulting in larger residual particles after the humidity decreases, but that would
7 not contribute to the backscatter – humidity relationship that is the core of the argument in the
8 paper.

9 **R: We agreed with reviewer’s concerns and deleted this sentence accordingly. To make the**
10 **issue more clearly, we added the following sentences to the last second paragraph of Sect. 1:**
11 *‘New particle formation and growth of particles by accretion of additional low volatility materials*
12 *(e.g., H₂SO₄) tend to be an irreversible but slow progress due to limited amount of condensable*
13 *gases, In contrast, hygroscopic growth of particles is a dynamic and typically reversible process,*
14 *and may affect the size of particles and its variation in the ATAL more remarkably in a relatively*
15 *short time since sufficient amount of water vapor can be frequently lofted to the UTLS via deep*
16 *convection during the Asian monsoon [Fu et al., 2006]’.*

17
18 P3L14: ‘mechanism’ >> ‘mechanisms’

19 **R: Done.**

20
21 P3L15: ‘the coagulation...the nucleation’ >> ‘coagulation...nucleation’

22 **R: Done.**

23
24 P3L17: ‘Except for coagulation,’ >> ‘Compared with coagulation,’

25 **R: Done.**

26
27 P3L21: ‘the stratospheric aqueous’ >> ‘stratospheric aqueous’

28 **R: Done.**

29
30 P4L18: it would be better to list the years of the BATAL campaign than to say ‘More Recently’.

31 **R: We rewrote this sentence as ‘A series of balloon borne activities between 2014 and 2017’ as**
32 **suggested by the reviewer.**

33
34 P4L25: ‘the vertical profiles’ >> ‘vertical profiles’

35 **R: Done.**

36
37 P5L7: ‘of the Compact Optical Backscatter Aerosol Detector (COBALD) particle backscatter
38 sonde, the iMet and RS92 radiosonde, and the cryogenic frost-point hygrometer (CFH).’ >> ‘of a
39 Compact Optical Backscatter Aerosol Detector (COBALD) instrument, iMet and RS92
40 rediosondes, and a cryogenic frost-point hygrometer (CFH).’

41 **R: Done.**

42
43 P5L10: ‘flew at’ >> ‘rose with’ or ‘ascended at a rate of’

44 **R: Done.**

1
2
3
4
5
6
7
8
9
10
11
12
13
14
15
16
17
18
19
20
21
22
23
24
25
26
27
28
29
30
31
32
33
34
35
36
37
38
39
40
41
42
43
44

P5L12: 'ascending' >> 'ascent'

R: Done.

P5L22: delete 'follow'

R: Done.

P5L27: 'scatter' >> 'scattering'

R: Done.

P5L29: 'raw data the blue' >> 'raw data, the blue'

R: This sentence was deleted owing to our response to the reviewer's comment for P6L1.

P6L1: 'and the precision in an order of 1%' >> 'and a precision of approximately 1%'. Rosen and Kjome should be included in a discussion of instrument uncertainty since it, to the extent that the COBALD instrument and data treatment are functionally similar, provides a far more complete description of the instrument performance than is available in the COBALD references such as Vernier et al. (2015).

R: The reviewer's comments are very valuable. We added a description of the instrument performance to the first paragraph of Sect. 2.1 as 'Before flight, the signal from each backscatter sonde is compared with a dedicated set of four standard backscatter sondes maintained in Laramie. The repeatability of the relative calibration between backscatter sondes is about $\pm 1\%$. The absolute calibration is believed accurate to better than $\pm 3\%$. Since naturally occurring aerosol backscatter ratios may be quite low, especially in the blue channel, it is important to consider potential sources of error and uncertainty in the absolute values derived from the basic measurements themselves. In the blue channel, a conservative adjustment procedure has been made in the range of 0 to 4% to eliminate nonphysical average values occurring in the troposphere [Rosen et al., 1997]'

P7L10: the ATAL has been typically observed [e.g. Vernier et al. (2015)] to occupy a much narrower range of altitudes than is described here and shown Fig 1. The top here certainly extends far into the stratosphere, many km above the tropopause and into the altitude range of the Junge layer. To tie the analysis here to the ATAL it is important to discuss the nature of the layer observed during these measurements and how/why it differs so dramatically from other ATAL observations.

R: We appreciate the reviewer's suggestions (also from Reviewer #1) and add the corresponding statement about the enhanced aerosol layer from COBALD measurement.

'On February 13, 2014 the Mt. Kelud (8°S, 112°E) in Indonesia erupted, with a volcanic plume located near 18-21 km within the tropical stratosphere, which was detected 11 days after the eruption by the Cloud-Aerosol Lidar with Orthogonal Polarization (CALIOP) onboard the Cloud-Aerosol Lidar and Infrared Pathfinder Satellite Observation (CALIPSO) [Vernier et al, 2016]. Stratospheric aerosols were perturbed significantly by the Kelud volcanic plumes, especially the fresh ash plume in the southern hemisphere [Vernier et al, 2016; Sakai et al., 2016], The Kelud volcanic eruption might have negligible influence on the observed aerosols in the ATAL, since the

1 *ATAL began to form about four months after the Kelud eruption when the volcanic materials in the*
2 *troposphere might have vanished. On the other hand, CALIOP data analysis also showed that*
3 *sulfate components from the Kelud volcanic eruption, peaking at an higher altitude with a longer*
4 *residence time compared with the volcanic ashes, influenced aerosol optical depth (AOD) between*
5 *20°N and 20°S 18-25 km considerably three months after the eruption [Vernier et al, 2016]. It is*
6 *likely that sulfate aerosols from the Kelud eruption contributed to stratospheric background*
7 *aerosols above the ATAL and even in the Junge layer at slightly higher latitude, as indicated by our*
8 *COBALD measurements’.*

9

10 P9L12: ‘concentration’ should be ‘mixing ratio’ here and elsewhere (e.g. L14, L15, Fig 3 caption)

11 **R: Done.**

12

13 P9L15: ‘convection transport’ >> ‘convective transport’

14 **R: Done.**

15

16 P10L6: ‘dependency’ >> ‘dependence’

17 **R: Done.**

18

19

20

21

22

23

24

25

26

27

28

29

30

31

1
2
3
4
5
6
7
8
9
10
11
12
13
14
15
16
17
18
19
20
21
22
23
24
25
26
27
28
29
30
31
32

Observational evidence of particle

condensational hygroscopic growth in the UTLS over the Tibetan Plateau

Qianshan He^{1,2}, Jianzhong Ma³, Xiangdong Zheng³, Xiaolu Yan³, Holger
Vömel⁴, Frank G. Wienhold⁵, Wei Gao^{1,2}, Dongwei Liu^{1,2}, Guangming Shi⁶,
Tiantao Cheng⁷

¹Shanghai Meteorological Service, Shanghai, China

²Shanghai Key Laboratory of Meteorology and Health, Shanghai, China

³State Key Laboratory of Severe Weather & CMA Key Laboratory of Atmospheric
Chemistry, Chinese Academy of Meteorological Sciences, Beijing, China

⁴Earth Observing Laboratory, National Center for Atmospheric Research, Boulder, CO,
USA

⁵ETH Zurich, Institute for Atmospheric and Climate Science (IAC), CH-8092 Zurich,
Switzerland.

⁶Chongqing Institute of Green and Intelligent Technology, Chinese Academy of
Sciences, Chongqing, China

⁷Department of Atmospheric and Oceanic Sciences, Institute of Atmospheric Sciences,
Fudan University, Shanghai, China

Correspondence to: Jianzhong Ma (majz@cma.gov.cn)

Key Points:

1. Balloon-borne measurements show an enhanced aerosol layer consisting dominantly
of fine particles in the UTLS over the Tibetan Plateau.

2. Water vapor ~~plays an important role in the growth of these fine particles.~~
is important in determining the size, and therefore radiative properties, of the particles.

Abstract

We measured the vertical profiles of ~~aerosol~~ backscattering ratio (BSR) ~~with using~~
the balloon-borne, lightweight Compact Optical Backscatter Aerosol Detector
(COBALD) instruments above Linzhia balloon-borne lightweight COBALD at Linzhi,
located in the southeastern Tibetan Plateau, in the summer of 2014. An enhanced
aerosol layer in the upper troposphere/lower stratosphere (UTLS), with BSR (455

1 nm) >1.1 and BSR (940 nm) >1.4 , was observed. The Color Index (CI) of the enhanced
2 aerosol layer, defined as the ratio of aerosol backscatter ratios (ABSR) at wavelengths
3 of 940 nm and 455 nm, varied from 4 to 8, indicating the prevalence of ~~dominant~~-fine
4 particles with mode radius less than 0.1 μm . We find that except for the very small
5 particles (mode radius smaller than 0.04 μm) at low relative humidity ($\text{RH}_i < 40\%$), the
6 relatively large particles in the aerosol layer were generally very hydrophilic as their
7 size increased dramatically with relative humidity. This result indicates that water vapor
8 can play a very important role in increasing the size of ~~the formation of large amounts~~
9 ~~of~~-fine particles in the UTLS over the Tibetan Plateau. Our observations provide
10 observation-based evidence supporting that ~~the~~—aerosol particle
11 hygroscopic~~condensational~~ growth is an important process—factor influencing the
12 radiative properties of ~~for the~~ summer Asian Tropopause Aerosol Layer (ATAL) during
13 the Asian summer monsoon enhancement by increasing the size of the fine particles
14 over the Tibetan Plateau.

15
16 **Keywords:** ATAL, hygroscopic~~condensational~~ growth, COBALD, Tibetan Plateau

17 18 **1. Introduction**

19 The Asian Tropopause Aerosol Layer (ATAL) extends over a large area within the
20 Asian summer monsoon circulation and may significantly influence ozone, cirrus
21 clouds and global climate by chemical, micro-physical and radiative processes
22 [Gettelman et al., 2011; Vernier et al., 2011; Fadnavis et al., 2013; Thomason and
23 Vernier, 2013; Vernier et al., 2015]. Particles in the ATAL are likely to be lifted to the
24 lower stratosphere by the large-scale upward circulation within the south Asian
25 anticyclone [Park et al., 2007], and then influence the aerosol amount in the global
26 stratosphere significantly [~~Park et al., 2007~~]. Solomon et al. [2011] found that the
27 radiative forcing of increased aerosols in the global stratosphere from 2000 to 2010 is
28 $-0.1\text{W}\cdot\text{m}^{-2}$, which weakened the global warming effect from increasing greenhouse
29 gases concentrations.

1 In addition to the ~~elevated~~maximum concentration of aerosols found in the ATAL
2 as mentioned above, the concentrations of tropospheric trace gases (i.e., water vapor,
3 CO, CH₄ and HCN) are higher within the Asian summer monsoon anticyclone than in
4 surrounding regions, while the stratospheric trace gases (i.e, O₃, HNO₃ and HCl) are
5 lower [Park et al., 2004; Randel et al., 2010]. Actually, the ~~elevated~~maximum aerosol
6 concentration near the tropopause over the Tibetan Plateau has also been observed by
7 lidar and balloon borne measurements [Kim et al., 2003; Tobo et al., 2007; He et al.,
8 2014]. Li [2005] showed that the aerosol plume is detectable in the anticyclone around
9 the altitude of 150 hPa over the Tibetan Plateau through satellite observations and
10 model study.

11 ~~The formation mechanism of ATAL has not been fully understood mainly due to~~
12 ~~sparse in situ measurements. Sources and formation mechanism of aerosols in the UTLS,~~
13 ~~especially over the tropics, have been studied over the past decades. [Frey et al., 2011]~~
14 ~~proposed that nucleation—New particle formation events can occur~~ at very low
15 temperatures accompanied by the outflow of convective systems, ~~as observed in the~~
16 ~~West African Monsoon [Frey et al., 2011]. could be dominant process in the production~~
17 ~~of ATAL. Vernier et al. [2015] found that there is a one-month phase lag of the aerosol~~
18 ~~scattering ratio from the Cloud Aerosol Lidar with Orthogonal Polarization (CALIOP)~~
19 ~~onboard the Cloud Aerosol Lidar and Infrared Pathfinder Satellite Observation~~
20 ~~(CALIPSO) after the phase of relative humidity with respect to ice (RH_i) from the~~
21 ~~Microwave Limb Sounding (MLS) at the beginning of the convective period~~
22 ~~(May/June), possibly due to the growth of the nanometric particles to the larger particles~~
23 ~~that can be detected by satellites.—~~

24 Both condensation and coagulation contribute to the particle growth, even though these
25 two processes are triggered by different mechanisms. Model studies have shown that
26 ~~the~~coagulation is more important than ~~the~~nucleation in the control of the number
27 concentration of fine particles (with diameter larger than 10 nm) in the UTLS [English
28 et al., 2011; Pierce and Adams, 2009; Timmreck et al., 2010]. ~~Compared with~~Except
29 ~~for~~ coagulation, the effect of condensation on particle growth is less documented in
30 previous studies. Weigel et al. [2011] found that supersaturated gases, which can

1 nucleate to form neutral and charged molecular clusters, also condense onto pre-
2 existing aerosol particles ~~and cloud droplets~~. Earlier studies focusing on polar
3 stratospheric clouds (PSCs) over the winter poles demonstrated that ~~the~~ stratospheric
4 aqueous H₂SO₄ aerosol can absorb a large amount of gaseous HNO₃ and H₂O at
5 temperatures (about 200K) between the nitric acid trihydrate (NAT) and ice frost points
6 [Carslaw et al., 1994; Tabazadeh et al., 1994], leading to a steep increase in particle
7 volume. ~~Heterogeneous reactions are active on the extreme cold stratospheric aerosols~~
8 ~~and polar stratospheric clouds (PSCs) over the winter poles~~. These aerosols and PSCs
9 are composed either of supercooled ternary solution (STS) droplets
10 (HNO₃·H₂O·H₂SO₄), ice particles or solid hydrates (most likely NAT) and can grow to
11 larger particles that are easy to sediment [Voigt et al., 2008; Engel, 2013]. However,
12 unlike the studies about PSCs, the growth mechanism of the particles in the ATAL is
13 still poorly described vague due to the lack of sufficient observations.

14 In-depth investigations on the aerosol size distribution, chemical composition and
15 growth process are needed for a better understanding of the characteristics and
16 formation mechanism of ATAL. It is difficult to obtain much more information merely
17 by means of remote sensing measurements, such as satellite and lidar, because those
18 sensors are not sensitive to ultra-fine particles. In such case, balloon and/or air borne *in*
19 *situ* measurement provide an additional and even better tool for exploring the ATAL.
20 Using a balloon-borne optical particle counter at Lhasa, China, Tobo et al. (2007)
21 measured the vertical profiles of aerosols and found occurrences of relatively high
22 number concentrations of sub-micron size aerosols near the tropopause region during
23 the Asian summer monsoon period. They considered that the enhanced aerosol layer in
24 the UTLS connected closely with the transportation of water vapor from the Asian
25 summer monsoon. An increased amount of water vapor was found in the UTLS within
26 the Asian summer monsoon anticyclone (Bian et al., 2012; Li et al., 2017). ~~Recently, a~~
27 ~~climate model simulation demonstrated that the abundant anthropogenic aerosol~~
28 ~~precursor emissions from Asia coupled with rapid vertical transport associated with~~
29 ~~monsoon convection could lead to significant particle formation in the upper~~

1 ~~troposphere within the ASM anticyclone (Yu et al., 2017). More Recently, a~~ series
2 of balloon borne activities between 2014 and 2017 over India and Saudi Arabia during
3 the Balloon Measurements of the Asian Tropopause Aerosol Layer (BATL)
4 campaigns revealed that the ATAL is composed of mostly small ($r < 0.25 \mu\text{m}$) liquid
5 ($\sim 80\% - 95\%$) aerosols with the dominant composition of nitrate (Vernier et al., 2017).
6 New particle formation and growth of particles by accretion of additional low volatility
7 materials (e.g., H_2SO_4) tend to be an irreversible but slow progress due to limited
8 amount of condensable gases. In contrast, hygroscopic growth of particles is a dynamic
9 and typically reversible process, and may affect the size of particles and its variation in
10 the ATAL more remarkably in a relatively short time since sufficient amount of water
11 vapor can be frequently lofted to the UTLS via deep convection during the Asian
12 monsoon [Fu et al., 2006].

13 As part of the project Tibetan Ozone, Aerosol and Radiation (TOAR) [see More
14 Information on ACP Special Issue, available at: [http://www.atmos-chem-](http://www.atmos-chem-phys.net/special_issue331.html)
15 [phys.net/special_issue331.html](http://www.atmos-chem-phys.net/special_issue331.html)], ~~the~~ vertical profiles of aerosols over the southeastern
16 Tibetan Plateau were measured in June and July of 2014. In this paper, we present the
17 results from balloon borne radiosonde measurements, and investigate the ~~contribution~~
18 effect of ~~condensational hygroscopic growth by gas to particle conversion processes to~~
19 on the observed ~~high concentrations~~ sizes and optical properties of fine particles in the
20 UTLS over the Tibetan Plateau.

22 **2. Experiment**

23 The field experiment was carried out at the Linzhi Meteorological Bureau (29.67°
24 N, 94.33° E; 2992 m above sea levelMSL), located in the southeastern Tibetan Plateau,
25 from June 6 to July 31, 2014. During the field campaign, seven balloon sondes were
26 launched, with each sounding taking place at about 16:00 UTC on June 18 (case 1),
27 June 24 (case 2), July 6 (case 3), July 15 (case 4), July 21 (case 5), July 25 (case 6) and
28 July 30 (case 7), respectively. The balloon sonde payload was composed of ~~the a~~
29 Compact Optical Backscatter Aerosol Detector (COBALD) instrument ~~particle~~
30 backscatter sonde, ~~the i~~Met and RS92 radiosondes, and ~~the a~~ cryogenic frost-point

1 hygrometer (CFH). The payload was lifted by a 1600 g latex balloon, which flew
2 ascended at an ascent-rate of 5-7 m s⁻¹. Data were obtained from the launching point
3 until an altitude between 30 km to 35 km where the balloon generally burst. In this
4 study, only the ascending-ascent data are analyzed.

5 2.1 COBALD particle backscatter sonde

6 The lightweight COBALD, developed by Prof. Thomas Peter's group at ETH
7 Zurich, uses two high power light emitting diodes (LEDs) operating at 455nm (blue)
8 and 940nm (infrared) with a silicon detector averaging the light scattered back from
9 molecules or aerosols at angles centered near 173° for typically one-second time
10 periods [Rosen and Kjome, 1991; Wienhold, 2012; Cirisan et al., 2014]. COBALD
11 measurements are only carried out at local nighttime as daylight saturates the sensitive
12 detector. Before flight, the signal from each backscatter sonde is compared with a
13 dedicated set of four standard backscatter sondes maintained in Laramie. The
14 repeatability of the relative calibration between backscatter sondes is about ±1%. The
15 absolute calibration is believed accurate to better than ±3%. Since naturally occurring
16 aerosol backscatter ratios may be quite low, especially in the blue channel, it is
17 important to consider potential sources of error and uncertainty in the absolute values
18 derived from the basic measurements themselves. In the blue channel, a conservative
19 adjustment procedure has been made in the range of 0 to 4% to eliminate nonphysical
20 average values occurring in the troposphere [Rosen et al., 1997].

21 Backscatter ratios (BSR) at two wavelengths are retrieved from COBALD
22 measurement, which is defined as follow,

$$23 \quad BSR = \frac{\beta_a + \beta_m}{\beta_m} = \frac{N_a \cdot \sigma_a + N_m \cdot \sigma_m}{N_m \cdot \sigma_m} \quad (1)$$

24 where β denotes backscatter coefficient, N the number concentration, and σ the
25 backscatter cross section. The subscripts a and m indicate contributions from aerosol
26 particles and air molecules, respectively. The backscatter cross section for air molecules
27 can be calculated from Rayleigh scattering theory and the number concentration for air
28 molecules is derived from atmospheric pressure and temperature measured by the
29 radiosonde. ~~From the COBALD raw data the blue and infrared backscatter ratio of each~~

1 ~~individual flight profile was derived with an accuracy of 5 % and the precision in an~~
2 ~~order of 1% [Vernier et al., 2015].~~ The backscattering cross section for aerosol particles
3 can be calculated from Mie scattering theory for a specified effective radius. The
4 aerosol backscatter ratio (ABSR) is defined as,

$$5 \quad ABSR = \frac{\beta_a}{\beta_m} = BSR - 1 \quad (2)$$

6 The ABSR values at two wavelengths are used to calculate the Color Index [CI,
7 Rosen et al., 1997], which is defined as the ABSR at 940 nm divided by the ABSR at
8 455 nm. The CI is proportional to the ratio of the backscatter cross sections at 940 and
9 455 nm, and hence it can provide an estimate of the particle size. Assuming an index
10 of refraction of 1.45 with 75% sulfate and a typical lognormal size distribution of the
11 stratospheric aerosols [Rosen and Kjome, 1991], the backscatter cross sections σ_a at the
12 wavelengths used by COBALD are calculated by Mie theory, and further the CI as a
13 function of the mean radius of total aerosol particles is derived. Because no information
14 on standard deviation of the lognormal distribution is available, the possible lower and
15 upper limits of the standard deviation are assumed to be 1.8 and 2.2 [Deshler et al.,
16 2003]. By comparing the observed CI with the calculated one for different standard
17 deviations, the range of possible mean radius can be obtained, and the number
18 concentration and further volume concentration for aerosol particles can be retrieved
19 from the observed ABSR according to the Equation (1).

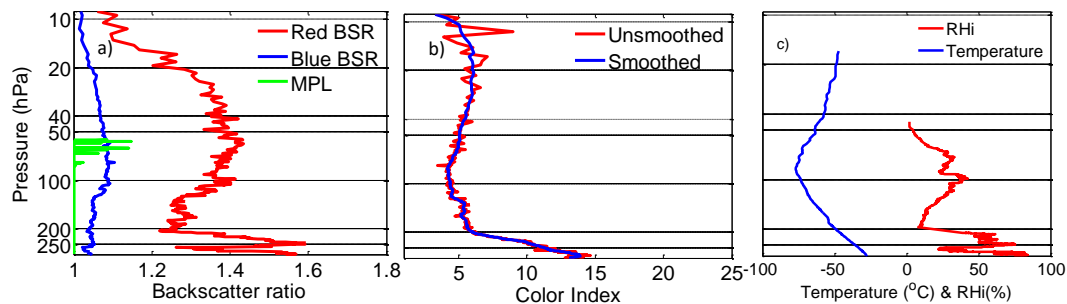
20 **2.2 Radiosonde observations**

21 In this study we use the air temperature profiles from the RS92 radiosondes with
22 an uncertainty of $\pm 0.2^\circ\text{C}$ below 100 hPa and $\pm 0.3^\circ\text{C}$ between 100 and 20 hPa. The
23 profiles of water vapor are obtained from CFH measurements. The CFH is a
24 microprocessor-controlled instrument with a lightweight of 400 g, and it uses a
25 cryogenic liquid as cooling agent and operates based on the chilled-mirror principle
26 [Vömel et al., 2007a]. The uncertainty of frost point or dew point measured by the CFH
27 is smaller than 0.2 K. Correspondingly, the uncertainty in relative humidity is estimated
28 to be 2 % for measurement in the lower troposphere and 5 % in the tropical tropopause
29 region [Vömel et al., 2016]. As a standard for water vapor measurements, CFH has

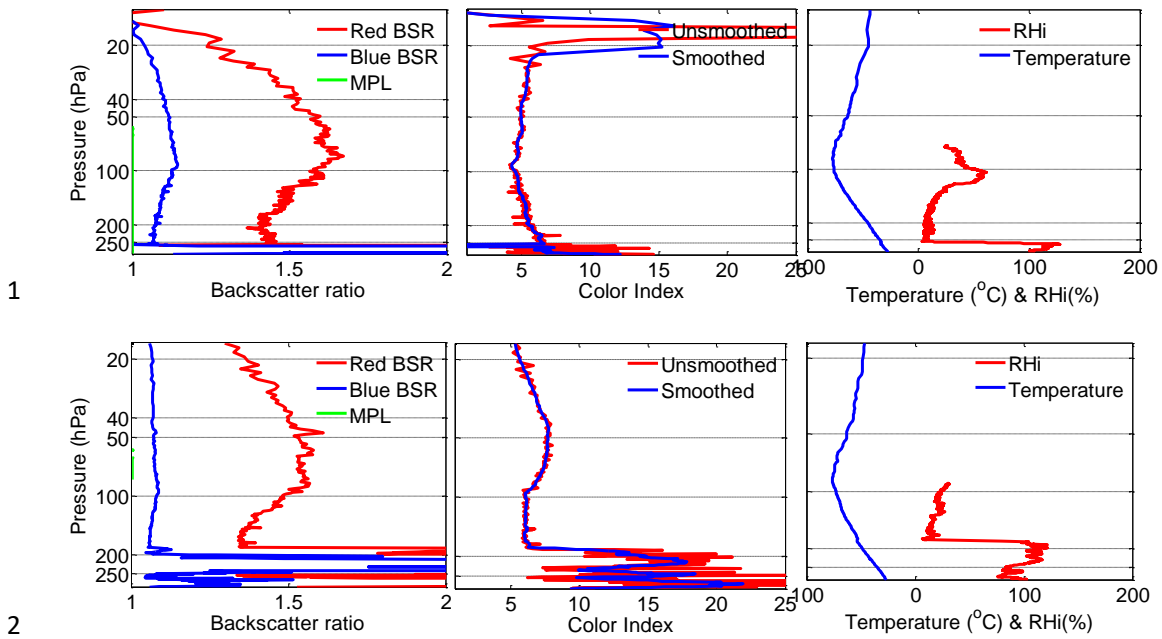
1 been used in numerous intercomparison experiments, such as the validation of Aura
 2 Microwave Limb Sounder (MLS) water vapor products, globally [Vömel et al., 2007b]
 3 and specifically over the Tibetan Plateau [Yan et al., 2016].
 4

5 3. Results and discussion

6 Figure 1 shows the BSR profiles at two wavelengths and calculated CI profiles
 7 from COBALD measurement, as well as the profiles of temperature and RH over ice
 8 respectively from RS92 and CFH measurement for three typical cases on June 18, July
 9 15 and 25, 2014. The COBALD measurements suggest an enhanced aerosol layer (BSR
 10 (455 nm) >1.1 and BSR (940 nm) >1.4) extending from 200 hPa (~12 km) to 10hPa (~28
 11 km) with a maximum above the tropopause (90 hPa, ~17 km). The enhanced aerosol
 12 layer from COBALD measurement is a mixture of ATAL and the on-setting Junge
 13 Layer due to the signal above 50 hPa stemming from the Junge Layer but the maximum
 14 occurring in ATAL. The RH_i near the maximum of the enhanced aerosol layer varies
 15 from 30% to 40%, indicating that it is impossibly caused by cirrus cloud, which cannot
 16 persist at these dry conditions. ~~It should be noted that the volcanic eruption might have~~
 17 ~~negligible influence on the observed aerosol layers as no volcanic eruption occurred~~
 18 ~~during the experiment period. Additionally, the volcanic materials in the lower~~
 19 ~~stratosphere from the eruption of Mt. Kelud (Indonesia) on Feb 13th, 2014 gathered~~
 20 ~~mainly in the southern hemisphere [Vernier et al., 2016; Sakai et al., 2016], and had a~~
 21 ~~negligible effect on the observed aerosol layers over the Tibetan Plateau.~~ The calculated
 22 CI of the enhanced aerosol layer is around 5 (4–8), far below CI of cirrus cloud (being
 23 around 10 with the maximum value exceeding 20) at 250 hPa [Vernier et al., 2015].



24



3 **Fig. 1.** (a) Three cases of the backscattering ratio profile from COBALD and MPL
 4 measurements on June 18 (top), July 15 (middle) and July 25 (bottom), 2014. (b) The
 5 calculated CI profiles from the ABSR at two wavelengths. (c) Temperature and RHi
 6 profiles measured by the RS92 radiosonde and CFH, respectively.

7
 8 On February 13, 2014 the Mt. Kelud (8°S, 112°E) in Indonesia erupted, with a
 9 volcanic plume located near 18-21 km within the tropical stratosphere, which was
 10 detected 11 days after the eruption by the Cloud-Aerosol Lidar with Orthogonal
 11 Polarization (CALIOP) onboard the Cloud-Aerosol Lidar and Infrared Pathfinder
 12 Satellite Observation (CALIPSO) [Vernier et al, 2016]. Stratospheric aerosols were
 13 perturbed significantly by the Kelud volcanic plumes, especially the fresh ash plume in
 14 the southern hemisphere [Vernier et al, 2016; Sakai et al., 2016]. The Kelud volcanic
 15 eruption might have negligible influence on the observed aerosols in the ATAL, since
 16 the ATAL began to form about four months after the Kelud eruption when the volcanic
 17 materials in the troposphere might have vanished. On the other hand, CALIOP data
 18 analysis also showed that sulfate components from the Kelud volcanic eruption,
 19 peaking at an higher altitude with a longer residence time compared with the volcanic
 20 ashes, influenced aerosol optical depth (AOD) between 20°N and 20°S 18-25 km
 21 considerably three months after the eruption [Vernier et al, 2016]. It is likely that sulfate

1 [aerosols from the Kelud eruption contributed to stratospheric background aerosols](#)
 2 [above the ATAL and even in the Junge layer at slightly higher latitude, as indicated by](#)
 3 [our COBALD measurements.](#)

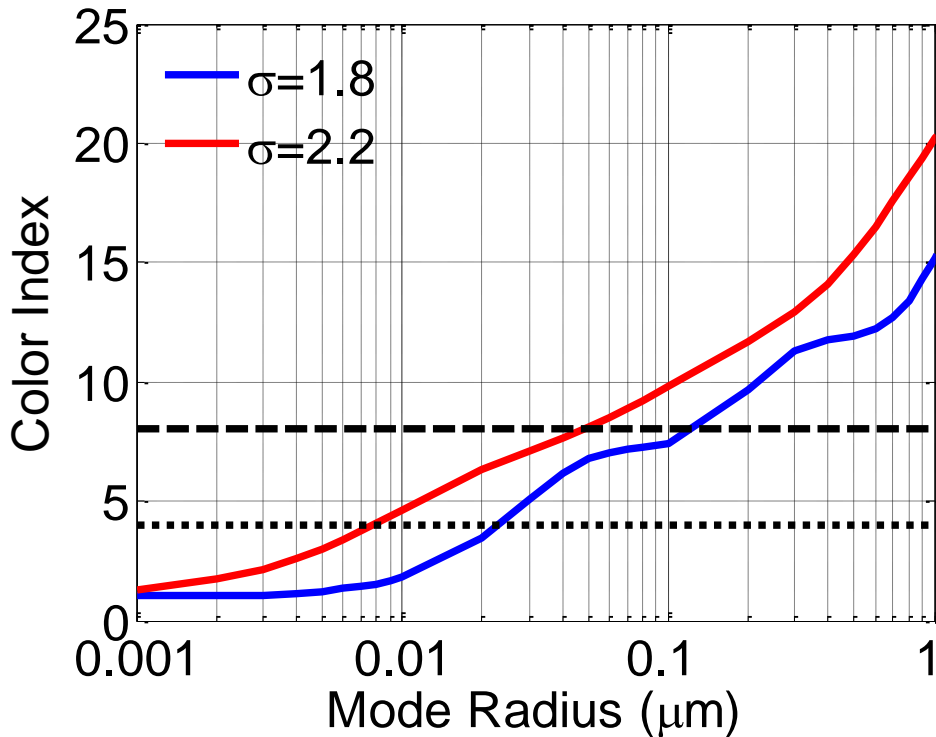
4 Pinnick et al. [1975] adopted a lognormal distribution with a mode radius of 0.0725
 5 μm and standard deviation (σ) of 1.86 to parameterize the background aerosols in the
 6 stratosphere. Rosen and Kjome [1991] suggested a mode radius between 0.04 and 0.06
 7 μm and σ value of ~ 2.0 - 2.2 for the 20-km stratospheric aerosol background layer. In
 8 this study, the CI as a function of mode radius was derived from Mie calculation using
 9 a lognormal distribution for different size of aerosols with standard deviations (σ) of
 10 1.8 and 2.2 respectively and the result is shown in Fig. 2. [The signal to noise ratio at](#)
 11 [the blue channel with respect to the molecular Rayleigh backscatter at tropopause](#)
 12 [conditions \(taken 100 hPa and 210 K\) is 220. Given the molecular backscatter](#)
 13 [coefficient of \$4.4e^{-7}\$ \(\$\text{sr}^{-1}\text{m}^{-1}\$ \) for 455 nm, this corresponds to a backscatter coefficient](#)
 14 [minimum detection limit of \$2e^{-9}\$ \(\$\text{sr}^{-1}\text{m}^{-1}\$ \), which is holding in general over the entire](#)
 15 [profile. To define an aerosol size limit, typical aerosol number densities need to be](#)
 16 [assumed: \$10\text{ cm}^{-3}\$ for stratospheric background and \$100\text{ cm}^{-3}\$ for the ATAL. The aerosol](#)
 17 [backscatter coefficients of different aerosol mode radius for the typical aerosol number](#)
 18 [densities are calculated by Mie theory and listed in Table 1. The results confirm that](#)
 19 [the particles with 100 nm radius are well detected under background conditions, which](#)
 20 [mainly contribute to the particulate backscatter ratio of approx. 0.01 and is always](#)
 21 [present. With increasing particle number density, the particles with 30 nm radius start](#)
 22 [to contribute to the particulate backscatter ratio \(\$> 2e^{-9}\text{ sr}^{-1}\text{m}^{-1}\$ \). Therefore, the lower](#)
 23 [size boundary that cannot be observed by COBALD due to the lack of scattering](#)
 24 [efficiency of small aerosols can be defined as 30 nm.](#)

25
 26 **Table 1** [The aerosol backscatter coefficients of different aerosol mode radius for the](#)
 27 [typical aerosol number densities.](#)

Mode Radius (nm)	10	30	100
$\beta_a@10\text{ cm}^{-3}$ ($\text{sr}^{-1}\text{ m}^{-1}$)	$1e^{-12}$	$3e^{-10}$	$2e^{-8}$

1

2 The CI increases monotonously from 1 to 15 with mode radius growing from 1 nm
3 to 1 μm . The CI of the enhanced aerosol layer from COBALD measurement usually
4 varied from 4 to 8 as indicated in this figure. With the assumed lognormal widths, the
5 measured CI imposes an upper limit of 100 nm on the particle radius. Therefore, we
6 conclude that the enhanced aerosol layer is composed of a large number of fine particles
7 with radius less than 0.1 μm . It has been documented that aerosols in the UTLS are
8 mainly composed of liquid inorganics with typical mode radii smaller than 0.1 μm
9 [Tobo et al., 2007]. Our observations in Linzhi are consistent with previous findings.



10

11 **Fig. 2.** CI as a function of mode radius from Mie calculation assuming an index of
12 refraction of 1.45 and a lognormal size distribution with the indicated standard
13 deviations (σ) of 1.8 and 2.2. The dotted and dashed lines represent the minimum (~ 4)
14 and maximum (~ 8) CI of the enhanced aerosol layer from COBALD measurement for
15 all cases.

16

17 The middle troposphere over the Tibetan Plateau is likely to act as a pipe for the

1 transport of water vapor from the marine boundary layer (i.e., Indian Ocean and South
2 China Sea) to the UTLS, leading to an increase of H₂O mixing ratio near the tropopause
3 [Fu et al., 2006; Lelieveld et al., 2007]. Figure 3(a) presents the CFH H₂O profiles from
4 110 hPa (~16 km ASL) to 90 hPa (~17.5 km ASL). It is noticed that H₂O ~~mixing~~
5 ~~ratio~~~~concentration~~ changes greatly in the vertical direction (3~12ppmv) for some cases.
6 The dehydration process results in minimum H₂O ~~mixing ratio~~~~concentration~~ just above
7 the altitude of each lowest temperature. Pronounced decrease of the H₂O ~~mixing~~
8 ~~ratio~~~~concentration~~ from 110 hPa to 90 hPa are attributed to ~~convection~~~~convective~~
9 transport of moist air parcels just occurring during the balloon flying periods. The three
10 relatively uniform H₂O profiles (on June 18, July 25 & 30) correspond to the well mixed
11 status of strong upward transport prior to the balloon-based measurements. The water
12 vapor cycle driven by synoptic-scale convection increases the possibility of ~~the~~
13 ~~condensation~~~~aerosol hygroscopic~~ growth ~~of aerosols~~ near the tropopause over the
14 Tibetan plateau. It has been estimated that the scattering ratio could increase by 10% to
15 50% with a water vapor mixing ratio enhancement from 3 ppmv to 6 ppmv [Vernier et
16 al., 2011].

17 Fig. 3(b) presents the variation of CI with RHi for all cases between 50 hPa and
18 150 hPa, the typical altitude range for the ATAL. The ~~dependency~~~~dependence~~ of CI
19 on RHi can be classified into three types according to the CI of dry aerosols, i.e. the
20 aerosols existing at very low relative humidity (e.g., RHi < 20%):

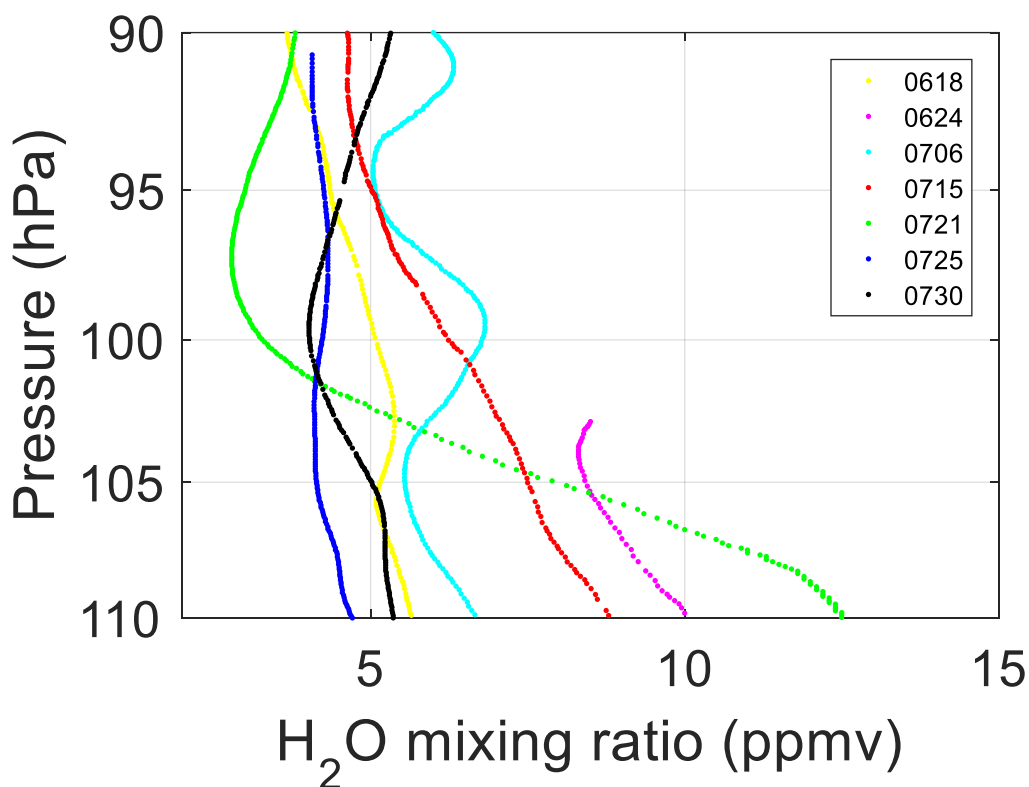
21 (1) When the CI of dry aerosol is larger than about 6, CI of the enhanced aerosol
22 layer shows an exponential growth with increasing RHi;

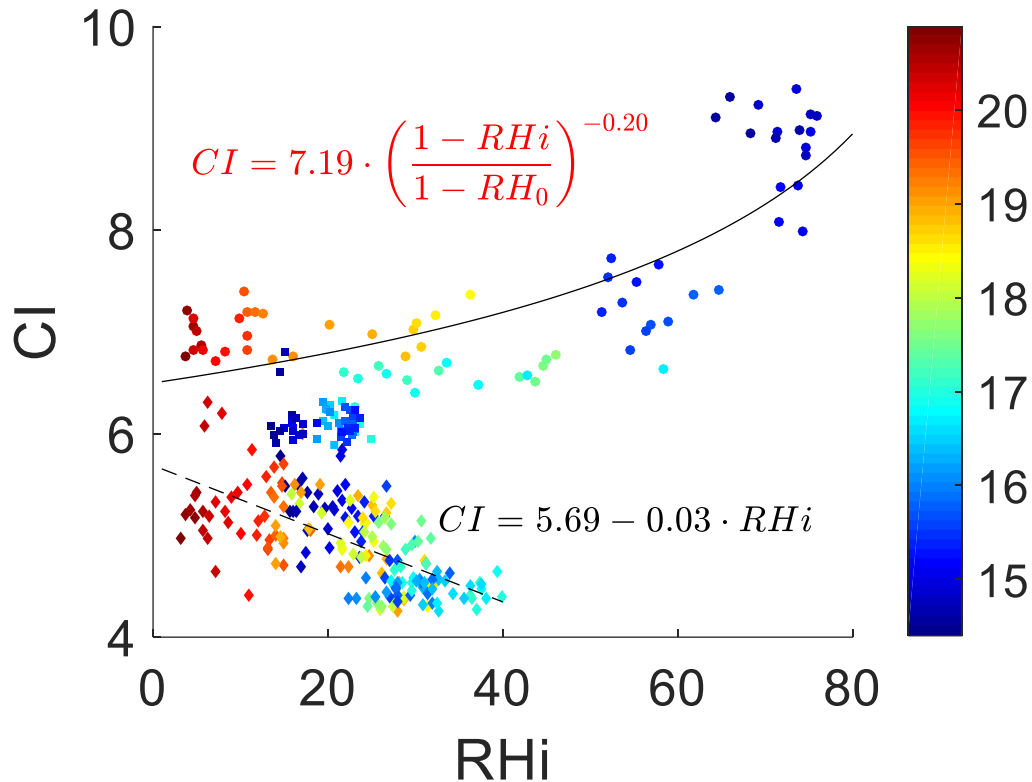
23 (2) When the CI of dry aerosol is smaller than about 6, CI of the enhanced aerosol
24 layer decreases with increasing RHi in a slope of -0.03;

25 (3) When the CI of dry aerosol is close to 6, it keeps almost constant with variation
26 of RHi.

27 As the CI can be regarded as an indicator of aerosol particle size, it can be inferred
28 that for those aerosol particles with large dry sizes (Type 1, i.e., CI > 6), increasing RHi
29 facilitates water vapor and other gaseous precursors to condense onto pre-existing
30 aerosol particles and then contribute to the particle growth. For those with small dry

1 sizes (Type 2 and Type 3, i.e., $CI \leq 6$), the situation appears to be more completed and
2 cannot be fully understood without more detailed information about aerosol chemical
3 composition and their gas precursors. Since all these aerosol particles were observed at
4 very low RH_i, well below 40% deliquescence relative humidity of most of the salts
5 (e.g., 40% for NH₄HSO₄) [Benson et al., 2009], the condensation-hygroscopic growth
6 of water vapor should have negligible effect on the growth-size of these particles under
7 this condition. New particle formation through the gas-to-particle conversion process,
8 which tends to become faster with increasing RH [Fountoukis and Nenes, 2007],
9 increases the number concentration, resulting in decrease of mode radius of bulk
10 aerosols. Therefore, the decrease of CI with RH_i (Type 2) indicates that new particle
11 formation might play an important role in the formation and prevalence of fine particles
12 in the UTLS over the Tibetan Plateau.





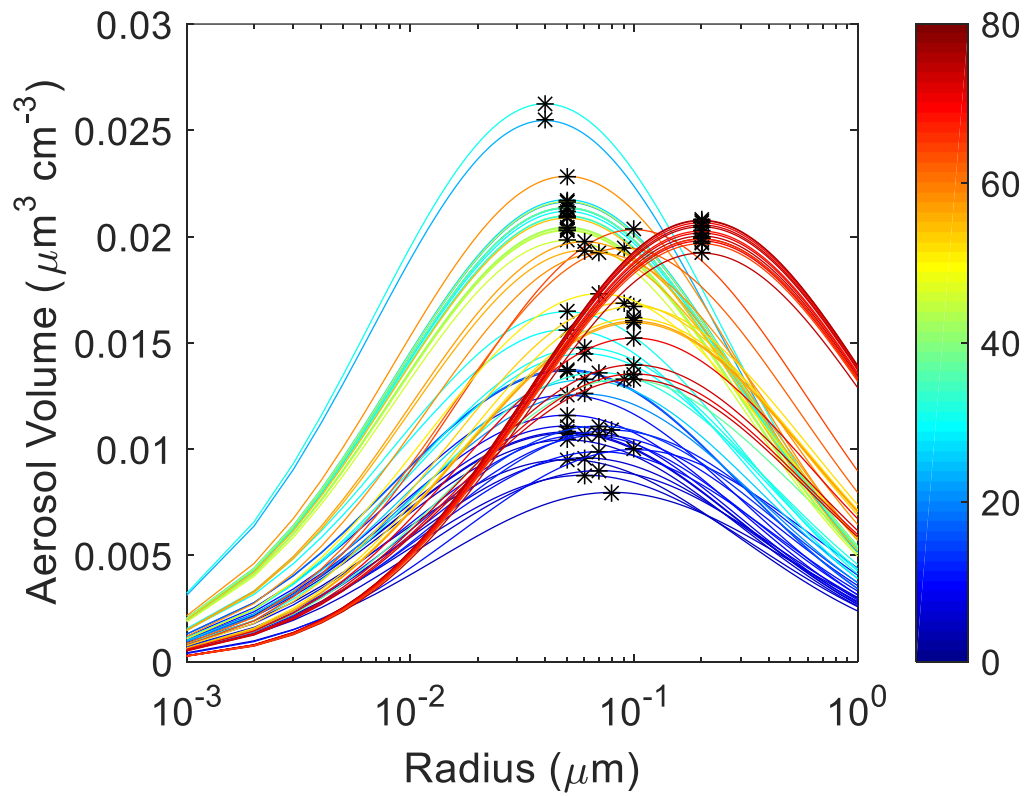
1

2 **Fig. 3.** (a) H₂O mixing ratio concentration from CFH measurements, and (b) the
 3 variation of CI with RH_i between 50 hPa and 150 hPa for all cases. The circles, square
 4 and diamond symbols are refer to those particles with CI of dry aerosol is larger than
 5 about 6, the squares close to 6 and the diamonds smaller than about 6, respectively. The
 6 altitude (in unit of km) of, where particles were measured, is marked with different
 7 color. The two fitted equations all exceeding the 99% significance level.

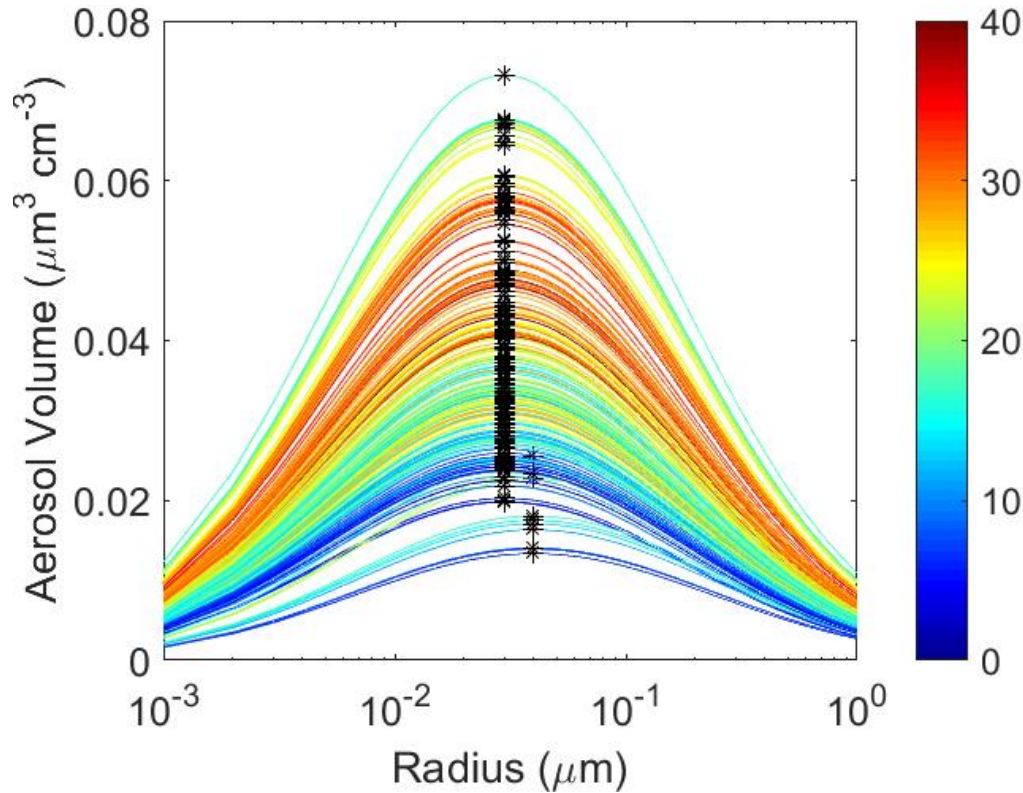
8

9 Based on the BSR and CI at the UTLS altitudes (50-150 hPa) from COBALD, we
 10 calculated the aerosol volume concentration in the enhanced aerosol layer for the two
 11 typical CI variation trend according to an assumption of lognormal size distribution
 12 with standard deviation of 1.8. The variation of aerosol volume concentration
 13 distributions with RH_i is shown in Fig. 4. It can be seen from Fig 4a that when RH_i is
 14 less than 60%, aerosol mode radius ranges mostly between 0.04 and 0.07 μm, and it
 15 increases steeply to 0.2 μm when RH_i is more than 60%. The aerosol volume
 16 concentrations are obviously high compared with those in dry condition, especially for
 17 those particles with a mode radius of 0.1 μm. For those aerosols with small initial dry

1 particle size (as shown in Fig 4b), accompanied by a mode radius decrease from 0.04
2 to 0.03 μm , the aerosol volume concentration increases by 4-5 times when RHi rises
3 from nearly zero to 40%, indicating that the number concentrations experience an
4 explosive growthincrease due to the formation of new particles.



5



1

2 **Fig. 4.** The variation of aerosol volume concentration distributions in the enhanced
 3 aerosol layer with RHi for (a) case 5 (July 21), and (b) the other cases corresponding to
 4 the CI<6 case (diamonds) ~~black dots~~ in Fig 3b. The color of each distribution represents
 5 RHi labeled on the color bar. The asterisk is mode radius of each distribution.

6

7 **4. Conclusions**

8 The vertical profiles of aerosol BSR measured over the southeastern Tibetan
 9 Plateau during summertime demonstrate an enhanced aerosol layer, consisting
 10 predominantly of fine particles with mode radius smaller than 0.1 μm, in the UTLS.
 11 The size of particles in the enhanced aerosol layer shows an exponential increase with
 12 increasing RHi when the CI of dry aerosols is larger than 6 (corresponding mode radius
 13 larger than 0.04 μm). It can be inferred that ~~for~~-increasing RHi leads to the more
 14 condensation of water vapor ~~and other gaseous precursor~~ onto pre-existing aerosol
 15 particles and contributes to the particle growth. For the CI of dry aerosols smaller than
 16 about 6 (i.e., mode radius smaller than 0.04 μm), the size of particles in the enhanced
 17 aerosol layer decreases with increasing RHi when RHi is below 40%, lower than typical

1 [aerosol deliquescence point](#). In this case, ~~more~~-new particle formation, which results in
2 a decrease of aerosol mode radius and [an](#) increase of number concentration, can play
3 an important role in the accumulation of large amounts of fine particles in the UTLS
4 over the Tibetan Plateau. [It must be borne in mind that the conclusions drawn from this](#)
5 [study are only based on 7 balloon flights so that general conclusions should be](#)
6 [established with caution. In fact,](#) ~~C~~chemical interactions involved in the stratosphere
7 troposphere exchange are complicated and further experimental and model studies are
8 needed to understand the nature and origin of [the](#) ATAL and its influence on global
9 atmospheric chemistry and climate.

11 **Author Contributions**

12 Qianshan He, Jianzhong Ma and Xiangdong Zheng designed the study. Holger Vömel
13 and Frank G. Wienhold respectively contributed to data quality control of COBALD
14 and CFH. Guangming Shi calculated Mie scattering parameters. Wei Gao, Dongwei
15 Liu and Tiantao Cheng contributed to data analysis, numerical experiments,
16 interpretation and paper writing. [Xiaolu Yan executed the in-situ balloon sondes](#)
17 [observation](#). Qianshan He did further analysis and interpreted the results. All authors
18 contributed to improve the manuscript.

19
20 *Acknowledgements.* This study was supported by the National Natural Science
21 Foundation of China (Grant No. 91637101, [91837311](#) and [91537213](#)) and the Shanghai
22 Science and Technology Committee Research Project (Grant No. 16ZR1431700). We
23 thank all TOAR team members and the staff from the Tibet Meteorological Service for
24 assisting our experiment work. We also thank Dr. Yutaka Tobo, whose useful
25 suggestions have greatly improved the paper.

28 **References**

29 Benson, D. R., Erupe, M. E., and Lee, S. H.: Laboratory-measured H₂SO₄-H₂O-NH₃
30 ternary homogeneous nucleation rates: Initial observations, *Geophys. Res. Lett.*,

1 36, 10.1029/2009gl038728, 2009.

2 Bian, J., Pan, L. L., Paulik, L., Vmel, H., Chen, H., and Lu, D.: In situ water vapor
3 and ozone measurements in Lhasa and Kunming during the Asian summer
4 monsoon, *Geophys. Res. Lett.*, 39(19), 19808, 2012.

5 Carslaw, K. S., Luo, B. P., Clegg, S. L., Peter, T. H., Brimblecombe, P., and Crutzen, P.
6 J.: Stratospheric aerosol growth and HNO₃ gas phase depletion from coupled
7 HNO₃ and water uptake by liquid particles, *Geophys. Res. Lett.*, 21, 2479 – 2482,
8 1994.

9 Cirisan, A., Luo, B. P., Engel, I., Wienhold, F. G., Krieger, U. K., Weers1, U., Romanens,
10 G., Levrat, G., Jeannet, P., Ruffieux, D., Philipona, R., Calpini, B., Spichtinger,
11 P., and Peter, T.: Balloon-borne match measurements of mid-latitude cirrus clouds,
12 *Atmos. Chem. Phys.*, 14, 7341–7365, 2014.

13 Deshler, T., Hervig, M. E., Hofmann, D. J., Rosen, J. M., and Liley, J. B.: Thirty years
14 of in situ stratospheric aerosol size distribution measurements from Laramie,
15 Wyoming (41N), using balloon-borne instruments, *J. Geophys. Res.*, 108,
16 doi:10.1029/2002JD002514, 2003.

17 Engel, I.: The Role of Heterogeneous Nucleation in Polar Stratospheric Cloud
18 Formation: Microphysical Modeling, ETH ZURICH, Doctor Dissertation, 2013.

19 English J. M., Toon, O. B., Mills, M. J., and Yu, F.: Microphysical simulations of new
20 particle formation in the upper troposphere and lower stratosphere, *Atmos. Chem.*
21 *Phys.*, 11, 9303–9322, 2011.

22 Fadnavis, S., Semeniuk, K., Pozzoli, L., Schultz, M. G., Ghude, S. D., Das, S., and
23 Kakatkar, R.: Transport of aerosols into the UTLS and their impact on the Asian
24 monsoon region as seen in a global model simulation, *Atmos. Chem. Phys.*,
25 13(17), 8771-8786, 2013.

26 Fountoukis, C., and Nenes, A.: ISORROPIA II: a computationally efficient
27 thermodynamic equilibrium model for K⁺ -Ca²⁺ -Mg²⁺ -NH⁴⁺ -Na⁺ -SO₄²⁻ -NO₃⁻
28 -Cl⁻ -H₂O aerosols, *Atmos. Chem. Phys.*, 7, 4639-4659, 10.5194/acp-7-4639-
29 2007, 2007.

30 ~~Frey, W., Borrmann, S., Kunkel, D., and Cairo, F.: In situ measurements of tropical~~

~~cloud properties in the West African monsoon: Upper tropospheric ice clouds, mesoscale convective system outflow, and subvisual cirrus, Atmos. Chem. Phys., 11, 5569–5590, doi:10.5194/acp-11-5569-2011, 2011.~~

Fu, R., Hu, Y., Wright, J. S., Jiang, J. H., Dickinson, R. E., Chen, M., Filipiak, M., Read, W. G., Waters, J. W., and Wu, D. L.: Short circuit of water vapor and polluted air to the global stratosphere by convective transport over the Tibetan Plateau, Proc. Natl. Acad. Sci. U. S. A., 103, 5664–5669, doi:10.1073/pnas.0601584103, 2006.

Gottelman, A., Hoor, P., Pan, L. L., Randel, W. J., Hegglin, M. I., and Birner, T.: The extratropical upper troposphere and lower stratosphere, Rev. Geophys., 49(3), RG3003, 2011.

He, Q. S., Li, C. C., Ma, J. Z., Wang, H. Q., Yan, X. L., Lu, J., Liang, Z. R., and Qi, G. M.: Lidar-observed enhancement of aerosols in the upper troposphere and lower stratosphere over the Tibetan Plateau induced by the Nabro volcano eruption, Atmos. Chem. Phys., 14, 1-9, 2014.

Kim, Y. S., Shibata, T., Iwasaka, Y., Shi, G. Y., Zhou, X. J., Tamura, K., and Ohashi, T.: Enhancements of aerosols near the cold tropopause in summer over Tibetan Plateau: Lidar and balloon borne measurements in 1999 at Lhasa, Tibet, China. Proc SPIE, 4893, 496-503, doi:10.1117/12.466090, 2003.

Lelieveld, J., Brühl, C., Jackel, P., Steil, B., Crutzen, P. J., Fischer, H., Giorgetta, M. A., Hoor, P., Lawrence, M. G., Sausen, R., and Tost, H.: Stratospheric dryness: model simulations and satellite observations, Atmos. Chem. Phys., 7, 1313-1332, doi:10.5194/acp-7-1313-2007, 2007.

Li, Q.: Trapping of Asian pollution by the Tibetan anticyclone: A global CTM simulation compared with EOS MLS observations, Geophys. Res. Lett., 32, L14826, doi:10.1029/2005GL022762, 2005.

Martinsson, B. G., Friberg, J., Andersson, S. M., Weigelt, A., Hermann, M., Assmann, D., Voigtländer, B. C. A. M., van Velthoven, P. J. F., and Zahn, A.: Comparison between CARIBIC aerosol samples analyzed by accelerator-based methods and optical particle counter measurements, Atmos. Meas. Tech., 7, 2581–2596, doi:10.5194/amt-7-2581-2014, 2014.

- 1 Li, D., Vogel, B., Bian, J., Müller, R., Pan, L. L., Günther, G., Bai, Z., Li, Q., Zhang,
2 J., Fan, Q., and Vömel, H.: Impact of typhoons on the composition of the upper
3 troposphere within the Asian summer monsoon anticyclone: the SWOP
4 campaign in Lhasa 2013, *Atmos. Chem. Phys.*, 17, 4657-4672, 10.5194/acp-17-
5 4657-2017, 2017.
- 6 Park, M., Randel, W. J., Kinnison, D. E., Garcia, R. R., and Choi, W.: Seasonal variation
7 of methane, water vapor, and nitrogen oxides near the tropopause: Satellite
8 observations and model simulations, *J. Geophys. Res.*, 109, D03302,
9 doi:10.1029/2003JD003706, 2004.
- 10 Park, M., Randel, W. J., Gettelman, A., Massie, S. T., and Jiang, J. H.: Transport above
11 the Asian summer monsoon anticyclone inferred from Aura Microwave Limb
12 Sounder tracers, *J. Geophys. Res.*, 112, D16309, doi:10.1029/2006jd008294,
13 2007.
- 14 Pierce, J. R., and Adams, P. J.: Can cosmic rays affect cloud condensation nuclei by
15 altering new particle formation rates? *Geophys. Res. Lett.*, 36, L09820,
16 doi:10.1029/2009GL037946, 2009.
- 17 Pinnick, R. G., Rosen, J. M., and Hofmann, D. J.: Stratospheric Aerosol Measurements
18 III: Optical Model Calculations, *J. Atmos. Sci.*, 33, 304-314, 1975.
- 19 Randel, W. J., Park, M., Emmons, L., and Pumphrey, H. C.: Asian monsoon transport
20 of pollution to the stratosphere, *Science*, 328, 611-613,
21 doi:10.1126/science.1182274, 2010.
- 22 Rosen, J., and Kjöme, N.: Backscatter_sonde: a new instrument for atmospheric aerosol
23 research, *Appl. Opt.*, 30, 1552–1561, 1991.
- 24 Rosen, J., Kjöme, N., and Liley, J.: Tropospheric aerosol backscatter at a midlatitude
25 site in the northern and southern hemispheres, *J. Geophys. Res.*, 102, D17, 21329-
26 21339, 1997.
- 27 [Sakai, T., Uchino, O., Nagai, T., Liley, B., Morino, I., and Fujimoto, T.: Long-term](#)
28 [variation of stratospheric aerosols observed with lidars over tsukuba, japan, from](#)
29 [1982 and lauder, new zealand, from 1992 to 2015, *J. Geophys. Res.*, 121\(17\),](#)
30 [10283-10293, 2016.](#)

- 1 Solomon, S., Daniel, J. S., Neely III, R. R., Vernier, J. P., Dutton, E. G., and Thomason,
2 L. W.: The persistently variable background stratospheric aerosol layer and global
3 climate change, *Science*, 333, 866-870, doi:10.1126/science.1206027, 2011.
- 4 Schlager, H., and Arnold, F.: Measurement of stratospheric gaseous nitric acid in the
5 Winter arctic vortex using a novel rocket-borne mass spectrometer method,
6 *Geophys. Res. Lett.*, 17, 433–436, 1990.
- 7 Tabazadeh, A., Turco, R. P., and Jacobson, M. Z.: A model for studying the composition
8 and chemical effects of stratospheric aerosols, *J. Geophys. Res.*, 99, 12897-12914,
9 1994.
- 10 Thomason, L. W., and Vernier, J. P.: Improved SAGE II cloud/aerosol categorization
11 and observations of the Asian tropopause aerosol layer: 1989-2005, *Atmos. Chem.*
12 *Phys.*, 13, 4605-4616, doi:10.5194/acp-13-4605-2013, 2013.
- 13 Timmreck, C., Graf, H. F., Lorenz, S. J., Niemeier, U., Zanchettin, D., Matei, D.,
14 Jungclaus, J. H., and Crowley, T. J.: Aerosol size confines climate response to
15 volcanic super-eruptions, *Geophys. Res. Lett.*, 37, L24705,
16 doi:10.1029/2010GL045464, 2010.
- 17 Tobo, Y., Iwasaka, Y., Shi, G. Y., Kim, S., Ohashi, T., Tamura, K., and Zhang, D. Z.:
18 Balloon-borne observations of high aerosol concentrations near the summertime
19 tropopause over the Tibetan Plateau, *Atmos. Res.*, 84, 233-241, doi:
20 10.1016/j.atmosres.2006.08.003, 2007.
- 21 Vernier, J. P., Thomason, L. W., and Kar, J.: CALIPSO detection of an Asian tropopause
22 aerosol layer, *Geophys. Res. Lett.*, 38, L07804, doi:10.1029/2010GL046614,
23 2011.
- 24 Vernier, J. P., Fairlie, T. D., Natarajan, M., Wienhold, F. G., Bian, J., Martinsson, B.
25 G., Crumeyrolle, S., Thomason, L. W., and Bedka, K. M.: Increase in upper
26 tropospheric and lower stratospheric aerosol levels and its potential connection
27 with Asian pollution, *J. Geophys. Res. Atmos.*, 120, 1608–1619,
28 [doi:10.1002/2014JD022372](https://doi.org/10.1002/2014JD022372), 2015.
- 29 [Vernier, J. P., Fairlie, T. D., Deshler, T., Natarajan, M., Knepp, T., and Foster, K.: In](#)

1 [situ and space - based observations of the kelud volcanic plume: the persistence](#)
2 [of ash in the lower stratosphere, J. Geophys. Res. Atmos., 121\(18\), 11104-11118,](#)
3 [2016.](#)

4 Vernier, J. P., Fairlie, T. D., Deshler, T., Kumar, B. S., Natarajan, M., Pandit, A. K.,
5 Akhil Raj, S. T., Hemanth Kumar, A., Jayaraman, A., Singh, A., Rastogi, N.,
6 Sinha, P. R., Kumar, S., Tiwari, S., Wegner, T., Baker, N., Vignelles, D.,
7 Stenchikov, G., Shevchenko, I., Smith, J., Bedka, K., Kesarkar, A., Singh, V.,
8 Bhate, J., Ravikiran, V., Durga Rao, M., Ravindrababu, S., Patel, A., Vernier, H.,
9 Wienhold, F. G., Liu, H., Knepp, T. N., Thomason, L., Crawford, J., Ziemba, L.,
10 Moore, J., Crumeyrolle, S., Williamson, M., Berthet, G., Jégou, F., and Renard,
11 J. B.: BATAL: The Balloon measurement campaigns of the Asian Tropopause
12 Aerosol Layer. Bulletin of the American Meteorological Society, BAMS-D-17-
13 0014.1, 2017.

14 Voigt, C., Schlager, H., Roiger, A., Stenke, A., de Reus, M., Borrmann, S., Jensen, E.,
15 Schiller, C., Konopka, P., and Sitnikov, N.: Detection of reactive nitrogen
16 containing particles in the tropopause region – evidence for a tropical nitric acid
17 trihydrate (NAT) belt, Atmos. Chem. Phys., 8(24), 7421-7430, doi:10.5194/acp-
18 8-7421-2008, 2008.

19 Vömel, H., Selkirk, L., Miloshevich, J., Valverde-Canossa, J., Valdes, J., and Diaz, J.:
20 Radiation Dry Bias of the Vaisala RS92 Humidity Sensor, J. Atmos. Ocean. Tech.,
21 24, 953–963, 2007a.

22 Vömel, H., Barnes, J. E., Forno, R., Fujiwara, M., Hasebe, F., Iwasaki, S., Kivi, R.,
23 Komala, N., Kyrö, E., Leblanc, T., Morel, B., Ogino, S. Y., Read, W. G., Ryan, S.
24 C., Saraspriya, S., Selkirk, H., Shiotani, M., Valverde Canossa, J., and Whiteman,
25 D. N.: Validation of Aura Microwave Limb Sounder water vapor by balloon-
26 borne Cryogenic Frost point Hygrometer measurements, J. Geophys. Res.,
27 112(D24), doi:10.1029/2007JD008698, 2007b.

28 Vömel, H., Naebert, T., Dirksen, R., and Sommer, M.: An update on the uncertainties
29 of water vapor measurements using cryogenic frost point hygrometers, Atmos.
30 Meas. Tech., 9, 3755-3768, doi:10.5194/amt-9-3755-2016, 2016.

- 1 Weigel, R., Borrmann, S., Kazil, J., Minikin, A., Stohl, A., Wilson, J. C., Reeves, J. M.,
2 Kunkel, D., de Reus, M., Frey, W., Lovejoy, E. R., Volk, C. M., Viciani, S.,
3 D'Amato, F., Schiller, C., Peter, T., Schlager, H., Cairo, F., Law, K. S., Shur, G.
4 N., Belyaev, G. V., and Curtius, J.: In-situ observations of new particle formation
5 in the tropical upper troposphere: The role of clouds and the nucleation
6 mechanism, *Atmos. Chem. Phys.*, 11, 9983–10010, doi:10.5194/acp-11-9983-
7 2011, 2011.
- 8 Wienhold, F. G.:
9 http://www.iac.ethz.ch/groups/peter/research/Balloon_soundings/COBALD_sensor,
10 COBALD Data Sheet, 2012.
- 11 Yan X. L., Wright, J. S., Zheng, X. D., Livesey, N., Vömel, H., and Zhou, X. J.:
12 Validation of Aura MLS retrievals of temperature, water vapour and ozone in the
13 upper troposphere and lower–middle stratosphere over the Tibetan Plateau during
14 boreal summer, *Atmos. Meas. Tech.*, 9, 3547-3566, doi:10.5194/amt-9-3547-
15 2016, 2016.
- 16 Yu P., Rosenlof, K. H., Liu, S., Telg, H., and Gao, R. S.: Efficient transport of
17 tropospheric aerosol into the stratosphere via the Asian summer monsoon
18 anticyclone. *Proc. Nation. Acad. Sci.*, 114(27): 6972-6977, 2017.